



1 **Ice nucleating particle concentrations unaffected by**  
2 **urban air pollution in Beijing, China**

3 Jie Chen<sup>1</sup>, Zhijun Wu<sup>1</sup>, Stefanie Augustin-Bauditz<sup>2</sup>, Sarah Grawe<sup>2</sup>, Markus Hartmann<sup>2</sup>,

4 Xiangyu Pei<sup>3</sup>, Zirui Liu<sup>4</sup>, Dongsheng Ji<sup>4</sup>, Heike Wex<sup>2</sup>

5 <sup>1</sup> State Key Joint Laboratory of Environmental Simulation and Pollution Control, College of  
6 Environmental Sciences and Engineering, Peking University, 100871, Beijing, China.

7 <sup>2</sup> Leibniz Institute for Tropospheric Research, 04318, Leipzig, Germany.

8 <sup>3</sup> Department of Chemistry and Molecular Biology, University of Gothenburg, 41296, Gothenburg,  
9 Sweden.

10 <sup>4</sup> State Key Laboratory of Atmospheric Boundary Layer Physics and Atmospheric Chemistry, Institute  
11 of Atmospheric Physics, Chinese Academy of Sciences, 100029, Beijing, China.

12 *Corresponding author:* Zhijun Wu ([zhijunwu@pku.edu.cn](mailto:zhijunwu@pku.edu.cn))

13 **Key Points:**

14 Ice nucleation

15 Urban aerosol

16 Immersion mode



## 17 Abstract

18 Exceedingly high levels of  $PM_{2.5}$  with complex chemical composition occur frequently in China. It has  
19 been speculated if anthropogenic  $PM_{2.5}$  may significantly contribute ice nucleating particles (INP).  
20 However, few studies have focused on the ice-nucleating properties of urban particles. In this work,  
21 two ice-nucleating droplet arrays have been used to determine the atmospheric number concentration of  
22 INP ( $N_{INP}$ ) in the range from  $-6\text{ }^{\circ}\text{C}$  to  $-25\text{ }^{\circ}\text{C}$  in Beijing. No correlations between  $N_{INP}$  and neither  $PM_{2.5}$   
23 nor black carbon mass concentrations were found, although both varied by more than a factor of 30  
24 during the sampling period. Similarly, there were no correlations between  $N_{INP}$  and either total particle  
25 number concentration or number concentrations for particles with diameters  $> 500\text{ nm}$ . Furthermore,  
26 there was no clear difference between day and night samples. All these indicate that Beijing air  
27 pollution did not increase or decrease INP concentrations in the examined temperature range above  
28 values observed in non-urban areas, hence, the background INP concentrations might not be  
29 anthropogenically influenced as far as urban air pollution is concerned, at least in the examined  
30 temperature range.

## 31 1 Introduction

32 Formation of the ice phase in clouds can be modulated by aerosols emitted from anthropogenic and  
33 natural sources (Morris et al., 2014; Murray et al., 2012; Rosenfeld et al., 2008) via heterogeneous ice  
34 nucleation (Pruppacher et al., 1998). This results in a significant impact on the cloud extent, lifetime,  
35 formation of precipitation, and radiative properties of clouds. Currently, four mechanisms are proposed  
36 for the heterogeneous ice nucleation in mixed-phase clouds: deposition ice nucleation, condensation  
37 freezing, immersion freezing, and contact freezing (Vali et al., 2015; Hoose and Möhler, 2012). It is  
38 under discussion if condensation freezing is different from immersion freezing on a fundamental level  
39 (Wex et al., 2014) and if at least some of the observed deposition ice nucleation can be attributed to pore  
40 condensation and freezing (Marcolli, 2014). For mixed-phase clouds, immersion freezing has been  
41 widely reported to be the most important ice nucleation mechanism (Ansmann et al., 2008; Murray et al.,  
42 2012; Westbrook and Illingworth, 2013). During the past decades, great efforts have been dedicated to  
43 understanding heterogeneous ice nucleation. However, it has become obvious that many fundamental  
44 questions in this field are still unsolved.



45 Numerous studies have attempted to quantify the ice nucleation ability of selected aerosol particles of a  
46 specific composition in immersion mode, such as dust (DeMott et al., 2015; Kaufmann et al., 2016;  
47 DeMott et al., 2003), marine (Wilson et al., 2015; DeMott et al., 2016; Alpert et al., 2011) and biological  
48 particles (Pummer et al., 2012; Hartmann et al., 2013; Fröhlich-Nowoisky et al., 2015). Biogenic  
49 particles in general have long been known to be able to induce ice nucleation at comparably high  
50 temperatures above  $-10^{\circ}\text{C}$  (e.g. Schnell and Vali, 1972). Recognized as the dominant INPs in mixed-  
51 phase clouds (Kamphus et al., 2010), particles from various mineral dusts were found to catalyse ice  
52 formation effectively in chamber experiments (Murray et al., 2012; Kanji et al., 2017). It has been widely  
53 accepted that biological particles can act as efficient INP, with some bacteria and fungi reported to  
54 possess the ability to arouse freezing at temperatures as high as  $-2^{\circ}\text{C}$  to  $-5^{\circ}\text{C}$  (Lundheim, 2002). Fungal  
55 spores (O'Sullivan et al., 2016; Pummer et al., 2015) and lichen (Moffett et al., 2015) are known to  
56 nucleate ice in the temperature range above  $-10^{\circ}\text{C}$ , while pollen (Augustin et al., 2013; Pummer et al.,  
57 2012) and ash particles (Grawe et al., 2016; Umo et al., 2015) may compete with mineral dust particles  
58 in terms of their ability to nucleate ice, albeit not in terms of their atmospheric abundance. Szyrmer and  
59 Zawadzki (1997), Hoose and Möhler (2012), Murray et al. (2012) and Kanji et al. (2017) are all reviews  
60 which give a more extensive overview over materials that can induce ice nucleation.

61 Although there has been a considerable number of studies aimed at understanding the ability of  
62 black carbon (BC)-containing particles acting as INP, the results are still controversial. Some studies  
63 show that BC-containing particles did not act as good INP (Schill et al., 2016; Chou et al., 2013). Chou  
64 et al. (2013) observed that soot particles from diesel engines and wood burning form ice at  $-40^{\circ}\text{C}$ , and  
65 unrealistically high relative humidity (RH) was needed for freezing initiation above this temperature.  
66 Schill et al. (2016) showed that neither fresh nor aged emissions from diesel engines contributed  
67 appreciably to atmospheric INP concentrations. However, some studies considered BC-containing  
68 particles as possible INPs (Cozic et al., 2008; Levin et al., 2016; Cozic et al., 2006). Observation of  
69 abundant BC in ice particle residuals in field experiments suggested that some BC-containing particles  
70 may preferentially act as INP (Cozic et al., 2008). In the experiments conducted by Levin et al. (2016),  
71 emissions of different types of biomass fuel produced measurable concentrations of INPs ( $0.1\text{-}10\text{ cm}^{-3}$ )  
72 associated with higher BC concentration accounting for about 0-70%. Determination of ice nucleating  
73 properties of physically and chemically aged soot particles suggests that the heterogeneous ice nucleation



74 activity of freshly emitted diesel soot particles is sensitive to some of the aging processes (Kulkarni et  
75 al., 2016).

76 In the atmosphere of urban areas with dense population, various sources and complex aging  
77 transformations (such as coagulation, condensation of vapor, chemical reaction) of particles can be found.  
78 Particularly, urban aerosol may be rich in BC-containing particles resulting from anthropogenic activities,  
79 such as fossil fuel combustion and biomass burning (Bond et al., 2013), which were speculated to play a  
80 role for the formation of ice in clouds (Kanji et al., 2017). However, the ice nucleating properties of  
81 particles produced in urban regions have rarely been the focus of previous studies.

82 Knopf et al. (2010) and Corbin et al. (2012) examined the ice nucleation activity of particles in the  
83 anthropogenically influenced atmospheric aerosol in Mexico City and Toronto, respectively, where in  
84 both studies the relative humidity at which measurements were made were below water vapor saturation  
85 (with respect to liquid water). Using filter samples, Knopf et al. (2010) state that organic particles  
86 included in their samples might potentially induce ice nucleation at conditions relevant to cirrus  
87 formation. Corbin et al. (2012) used a CFDC (Continuous-Flow Diffusion Chamber) operating at  $-33^{\circ}\text{C}$   
88 together with a particle mass spectrometer. Statistical limitations impeded a statistical sound analysis,  
89 but their data suggests that dust particles, particles from biomass burning and particles containing  
90 elemental carbon might be sources of INP at their experimental conditions. They explicitly encourage  
91 further studies of these particles types concerning their role as possible INP.

92 In general, burning of liquid fuels produces soot particles (i.e., particles that are mostly organic),  
93 while burning of solid material as e.g., biomass or coal will also produce ash particles which contain the  
94 inorganic components that made up the fuel. Umo et al. (2015) and Grawe et al. (2016) examined the ice  
95 activity of ash particles from wood and coal burning in the immersion mode and both find that these  
96 particles are ice active. In Grawe et al. (2016), ash particles with atmospherically relevant sizes of 300 nm  
97 were examined and the most active particles came from a sample of fly ash from a coal burning power  
98 plant, inducing immersion freezing below  $-22^{\circ}\text{C}$ . However, different ash samples showed different ice  
99 activities, and also large differences in the results between the methods used for the examination were  
100 described.

101 In the present study, we measured the ice nucleating activity of urban aerosols in parallel with BC  
102 and  $\text{PM}_{2.5}$  mass concentration and particle number concentrations in the atmosphere of the mega-city  
103 Beijing, which is frequently experiencing heavy pollution. During heavy haze episodes,  $\text{PM}_{2.5}$  mass



104 concentration can be several hundred micrograms per cubic meter and is composed of a complex mixture  
105 of different chemical components (organic matter, inorganic ions and black carbon) (Zheng et al., 2016).  
106 The goal of this project is to find out if anthropogenic sources which are dominant in the urban  
107 atmosphere significantly contribute to the local INP concentrations, focusing particularly on the ice  
108 nucleating ability of BC in urban aerosols.

## 109 **2 Materials and Methods**

### 110 **2.1 Sample collection and particle number measurement**

111 The sampling site for particle collection was on the roof of a six-floor building (about 30 m above  
112 ground level) on the campus of Peking University (39°59'20"N, 116°18'26"E), located in the north-  
113 western urban area of Beijing.

114 Particles with an aerodynamic diameter less than or equal to 2.5 micro-meters (PM<sub>2.5</sub>) were collected  
115 on quartz fiber (Whatman, 1851-865) and PTFE filters (Whatman, 7592-104) using a 4-channel sampler  
116 with 2.5µm impactors from 27<sup>th</sup> November 2016 to 1<sup>st</sup> December 2016 and 13<sup>th</sup> December 2016 to 22<sup>th</sup>  
117 December 2016. Daytime filters were collected from 8:00 am to 8:00 pm and nighttime filters were  
118 collected from 8:00 pm to 8:00 am with an air flow rate of 16.7 L min<sup>-1</sup>, resulting in a total volume of air  
119 sampled on each filter of ~12000 L. The quartz filters were treated before the sampling by heating them  
120 to 550 °C for 6 h. After sampling, all filters were kept at ≤ -18 °C during storage, and the INP analysis  
121 was done within 20 days, starting on 5th February in 2017.

122 A scanning mobility particle sizer (SMPS, TSI Inc., USA) system was used to obtain particle  
123 number distribution in the 3-700 nm (electrical mobility diameter) size range during the sampling period  
124 while an aerodynamic particle sizer (APS, TSI model 3321, TSI Inc., USA) measured particle number  
125 size distributions between 800 nm and 2.5µm (aerodynamic diameter). The APS results were transformed  
126 from aerodynamic diameter to Stokes diameter with a particle density of 1.5 g cm<sup>-3</sup> which were measured  
127 by a CPMA (centrifugal particle mass analyzer) and combined with the measured and inverted size  
128 distributions obtained from the SMPS. From these combined size distributions, we calculated the total  
129 particle number concentration of particles in the diameter range from 3nm to 2.5µm ( $N_{total}$ ) and number  
130 concentrations of particles larger than 500nm ( $N_{>500nm}$ ). When comparing with filter results, we use 12h-  
131 average values of  $N_{total}$  and  $N_{>500nm}$ , where the averages were always made from 8:00 am to 8:00 pm for



132 daytime data and from 8:00 pm to 8:00 am for nighttime data.  $N_{>500nm}$  was derived, as in general larger  
133 particles are expected to be more efficient INP, and also as this size range was selected in DeMott et al.  
134 (2010, 2015) to serve as a base for parameterizations of INP number concentrations.

135 Concentrations of BC were continuously measured by a multi-angle absorption photometer (5012  
136 MAAP, Thermo Fisher Scientific, Waltham, MA, USA) utilizing a 637 nm LED as a light source (Müller  
137 et al., 2011).

## 138 2.2 Chemical analysis

139 Two PTFE filters were always sampled in parallel, and while one was used for INP analysis, the  
140 other was selected for the total mass and water-soluble ion analysis.  $PM_{2.5}$  mass concentration was  
141 obtained with an analytical balance by the gravimetric method (Mettler Toledo AG285) (Yang et al.,  
142 2011). As for water-soluble inorganic compounds analysis, Guo et al. (2012) described the method for  
143 seven major ions ( $K^+$ ,  $Mg^{2+}$ ,  $Ca^{2+}$ ,  $NH_4^+$ ,  $NO_3^-$ ,  $SO_4^{2-}$  and  $Cl^-$ ) measured by ion-chromatograph (DIONEX,  
144 ICS-2500/2000) based on the usage of PTFE filters. Post-sampling, all filters were stored in the  
145 refrigerator at  $-18\text{ }^\circ\text{C}$  before analysis.

## 146 2.2 INDA and LINA analysis

147 Two devices called INDA (Ice Nucleation Droplet Array) and LINA (Leipzig Ice Nucleation  
148 Array) have been set up at the Leibniz Institute for Tropospheric Research (TROPOS) in Germany  
149 following the design described in Conen et al. (2012) and in Budke & Koop (2015), respectively.  
150 INDA was used to investigate the immersion freezing properties of the quartz fibre filter samples while  
151 LINA was used to test the particles on PTFE filters.

152 INDA consists of a thermostat (JULABO FP40) with a 16 L cooling bath. 96 circles (1mm in  
153 diameter each) of each quartz filter were cut out by a punch and immersed separately in the tubes of a  
154 PCR (Polymerase chain reaction) tray which each contained 50  $\mu\text{l}$  distilled water. While Conen et al.  
155 (2012) originally used separate Eppendorf Tubes®, the use of PCR trays for immersion freezing  
156 studies has been suggested before in Hill et al. (2016) and was adapted in the LINA set-up. The PCR  
157 trays were placed on a sample-holder and exposed to decreasing temperatures with a cooling rate of  
158 approximately  $1\text{ K min}^{-1}$  in the cooling bath down to  $-30\text{ }^\circ\text{C}$ . Real time images of the PCR trays were



159 recorded every 6 seconds by a CCD (Charge Coupled Device) camera. A flat light that was fixed at the  
160 bottom of the cooling bath helped to yield proper contrast between frozen and unfrozen droplets on the  
161 recorded pictures, so that frozen droplets could be identified according to the brightness change during  
162 the freezing process. A program recorded the current temperature of the cooling bath and related it to  
163 the real-time images from the CCD camera. The temperature in the PCR trays had been calibrated  
164 previously as described in section 1.1 of the appendix.

165 For the measurement of ice nucleating particles at lower temperature, LINA was built according  
166 to an optical freezing array named BINARY, which was described in detail by Budke & Koop (2015).  
167 PTFE filters collected during the same period as quartz fibre filters were used for LINA. Half of the  
168 PTFE filter of each day was immersed in 10 ml distilled water and shaken for 1 h to wash particles off.  
169 For each measurement, 90 droplets with the volume of 1  $\mu\text{l}$  were pipetted from the resulting suspension  
170 onto a thin hydrophobic glass slide (diameter 40 mm, thickness 0.13-0.16 mm, obtained from  
171 Marienfeld-superior), with each droplet being contained in a separate compartment. These  
172 compartments were round holes with diameters of 3 mm, drilled into an aluminium plate with a  
173 diameter of 40 mm and a thickness of 14 mm. Both, hydrophobic glass slide and the aluminium plate  
174 with the compartments were surrounded by an aluminium ring with an inner diameter of 40 mm, which  
175 acted to keep glass slide and aluminium plate in place. Slide, plate and ring were all arranged before  
176 the droplets were pipetted. A second thin glass slide was put on top of the plate so that the  
177 compartments were all separated from each other and that evaporation of the droplets was prevented.  
178 The droplets were cooled on a Peltier element with a cooling rate of 1 K  $\text{min}^{-1}$ . There was a thin oil  
179 (squalene) film between the hydrophobic glass slide and the Peltier element for optimal heat  
180 conductivity. The temperature on the glass slide had been determined previous to the experiments as  
181 described in section 1.2 of the appendix, and the temperature shift between that set on the Peltier  
182 element and that observed on the glass slide was accounted for in the data presented herein. The  
183 freezing process again was recorded by taking pictures with a CCD camera every 6 seconds and  
184 detecting the freezing based on a change in the reflectance of the droplets upon freezing.

185 As mentioned above, the temperature calibration for these two instruments is described in detail  
186 in the section 1.1 and 1.2 of the appendix. The background freezing signal of pure distilled water and  
187 circles cut from clean filters were tested as well. These results are shown in the section 2 of the  
188 appendix.



189 The measurements resulted in frozen fractions ( $f_{ice}$ ) as defined in Eq. (1):

$$190 \quad f_{ice} = \frac{N_{frozen}}{N_t} \quad (1)$$

191 where  $N_{frozen}$  is the number of frozen tubes or droplets at a certain temperature and  $N_t$  is the total  
192 number of tubes in PCR trays (i.e., 96) or droplets on the slides (i.e., 90).

193 The temperature dependent cumulative number concentration of INP ( $N_{INP}$ ) per volume of  
194 sampled air was calculated according to Eq. (2), similarly to Vali (1971) and Conen et al. (2012):

$$195 \quad N_{INP}(T) = -\frac{\ln(1-f_{ice}(T))}{V_{sampled}} \quad (2)$$

196 where  $N_{unfrozen}$  is the number of tubes or droplets still unfrozen (liquid) at a certain temperature, and  
197  $V_{sampled}$  is the volume of air converted to standard conditions (0°C and 1013hPa) from which the  
198 particles were collected that were suspended in each of the droplets in LINA or that were collected on  
199 each filter punch used for INDA measurements, respectively.

200 The chemical ion analysis in section 3.1 and the determination of the  $PM_{2.5}$  mass concentration  
201 was done at Peking University. The filters used for INP measurements were brought to TROPOS  
202 where then INP measurements were done. Filters were continuously cooled below 0°C in a portable ice  
203 box during transport.

## 204 **3 Results and Discussion**

### 205 **3.1 Severe $PM_{2.5}$ pollution in Beijing**

206 Fig. 1 shows the time series of  $PM_{2.5}$  mass concentrations and chemical composition during the  
207 sampling period. The  $PM_{2.5}$  mass concentration with a mean value of  $97.30 \pm 77.9 \mu\text{g m}^{-3}$  ranged from  
208  $6.54 \mu\text{g m}^{-3}$  up to  $273.06 \mu\text{g m}^{-3}$ . Here, the cases with  $PM_{2.5}$  above  $50 \mu\text{g m}^{-3}$  were defined as polluted  
209 days, whereas the rest was defined as clean days. On average, the sulfate, nitrate, and ammonia (SNA)  
210 accounted for around 35% of  $PM_{2.5}$  during the whole period with an obvious enhancement in polluted  
211 days (53%), indicating that secondary transformation could be one major contributor to the formation  
212 of particulate pollution. Dust particles are in the coarse mode, and only contribute little to the total  
213  $PM_{2.5}$  load (Lu et al., 2015; Li and Shao, 2009). In these studies,  $Ca^{2+}$  as a tracer for dust particles  
214 showed a low proportion in  $PM_{2.5}$ , suggesting that the dust particles also only contributed little to  $PM_{2.5}$   
215 during our observations as well.





216 During the sampling period, BC mass concentrations varied from  $0.50 \mu\text{g m}^{-3}$  on clean days up to  
217  $17.26 \mu\text{g m}^{-3}$  on polluted days. On average, the mean mass concentration of BC,  $7.77 \pm 5.23 \mu\text{g m}^{-3}$ ,  
218 accounted for about 13% of  $\text{PM}_{2.5}$ . During night time, BC concentrations were higher than those during  
219 daytime due to stronger diesel engine emissions and a lower boundary layer (Guo et al., 2012). Our  
220 previous studies showed that secondary and primary organic aerosols contributed to around 36% of  
221 non-refractory  $\text{PM}_1$  detected by an aerosols mass spectrometer during wintertime in the atmosphere of  
222 Beijing (Hu et al., 2017).

### 223 3.2 Particle number concentrations

224 Fig. 2 shows the time series of the total number concentration of particles from 3 nm up to  $2.5 \mu\text{m}$   
225 ( $N_{total}$ ) and the number concentration of particles larger than 500 nm ( $N_{>500nm}$ ), where  $N_{total}$  varied from  
226  $3 \cdot 10^3$ – $7 \cdot 10^4 \text{ cm}^{-3}$  and  $N_{>500nm}$  varied from 10 to  $4 \cdot 10^3 \text{ cm}^{-3}$ . Obviously, in the atmosphere of Beijing  
227 during the sampling period, small particles less than 500 nm account for a large fraction of the total  
228 particle number concentration, but during strong pollution events, also a large increase in  $N_{>500nm}$  is  
229 seen.

230 The 12h-averages of  $N_{>500nm}$  shown in the upper panel of Fig. 2 were used to determine INP  
231 number concentrations ( $N_{INP}$ ) at  $-16 \text{ }^\circ\text{C}$ , following parameterizations suggested by DeMott et al. (2010,  
232 2015) and shown as blue and green squares in the lower panel of Fig. 2, respectively. Mostly, the  
233 parameterization by DeMott et al. (2015) yields larger values and a larger spread, compared to the  
234 parameterization by DeMott et al. (2010), but naturally both follow the trends in  $N_{>500nm}$ . A correction  
235 factor of 3, as suggested in DeMott et al. (2015), was not applied, as this would simply increase all  
236 respective values by this factor, i.e., it will not change the results we discuss in the following.

237 Fig. 3(a) and Fig. 3(b) show  $N_{INP}$  as a function of temperature for INDA measurements. The lines  
238 are colour coded depending on the  $\text{PM}_{2.5}$  mass concentration (Fig. 3(a)) and 12h-average  $N_{>500nm}$  (Fig.  
239 3(b)) during the respective filter sampling, where each line (30 in total) represents an individual result  
240 of a filter. All filter samples had INP that were active at  $-12.5 \text{ }^\circ\text{C}$  and the highest freezing temperature  
241 was observed to be  $-6 \text{ }^\circ\text{C}$ . Overall,  $N_{INP}$  varied from  $10^{-3}$  to  $1 \text{ L}^{-1}$ . Already at a first glance, there is no  
242 clear trend in  $N_{INP}$  with  $\text{PM}_{2.5}$  mass concentration and 12h-average  $N_{>500nm}$ , indicating that the dominant



243 pollutants of urban atmosphere may not significantly contribute to INPs active down to roughly  $-16^{\circ}\text{C}$   
244 in an urban region.

245 To verify the results observed in INDA at lower temperatures,  $\text{PM}_{2.5}$  collected by PTFE filters in  
246 the same period were used for LINA which can test the ice nucleating properties of droplets down to  
247 below  $-20^{\circ}\text{C}$ . Washing particles off from the PTFE filters was more complete for some filters than for  
248 others. This showed in differently large deviations in  $N_{\text{INP}}$  from INDA and LINA measurements in the  
249 overlapping temperature range, where results determined from INDA were always similar to or higher  
250 than those from LINA as particle removal by washing the filters was frequently incomplete. While  
251 sampling on fibre filters with subsequent washing cannot be recommended in general, we decided to  
252 use a subset of the therewith obtained data. For our analysis, ten LINA measurements from different  
253 days were selected, for which the deviation factor ( $N_{\text{INP}}$  of INDA /  $N_{\text{INP}}$  of LINA) obtained from two  
254 methods in the overlapping temperature range was small, varying from 1.3 to 4.4. These data are  
255 shown in Fig. 3(c) and Fig. 3(d). The LINA data is represented by the dotted lines and the respective  
256 INDA data from the same sampling periods is represented by solid lines. In the temperature from  $-20^{\circ}\text{C}$   
257 to  $-25^{\circ}\text{C}$ , results of LINA also show no clear trend in  $N_{\text{INP}}$  with  $\text{PM}_{2.5}$  mass concentration and 12h-  
258 average  $N_{>500\text{nm}}$ , even though a lower temperature has been involved, extending our statement that  
259 urban pollution might not contribute to INP down to  $-25^{\circ}\text{C}$ .

### 260 3.3 Correlation of $N_{\text{INP}}$ with $\text{PM}_{2.5}$ , and BC mass concentration and particle number concentrations

261 There have been many studies carried out in field and laboratory focusing on the ice nucleating  
262 properties of BC particles, however with inconclusive results. Some held the view that BC is not an  
263 efficient ice nucleation active species (Kamphus et al., 2010; Schill et al., 2016), whereas some  
264 described BC particles as possible INPs (Cozic et al., 2008; Cozic et al., 2007).

265 Here we selected  $N_{\text{INP}}$  derived from INDA measurements at  $-16^{\circ}\text{C}$  and plotted them against BC  
266 (Fig. 4 (a)),  $\text{PM}_{2.5}$  mass concentrations (Fig. 4 (b)) and 12h-average values of  $N_{\text{total}}$  (Fig. 4 (c)),  $N_{>500\text{nm}}$   
267 (Fig. 4 (d)), and  $N_{\text{INP}}$  at  $-16^{\circ}\text{C}$  derived from DeMott et al. (2010) (Fig.4 (e)) and DeMott et al. (2015)  
268 (Fig.4 (f)). Our results discussed in the following, based on  $N_{\text{INP}}$  at  $-16^{\circ}\text{C}$ , are similarly valid for all  
269 other temperatures down to  $-25^{\circ}\text{C}$ .



270 Fig. 4(a) to (f) show that there was no clear trend between  $N_{INP}$  and any of the displayed  
271 parameters, be it BC or  $PM_{2.5}$  mass concentration or any of the 12h-average particle number  
272 concentrations. In the urban region of Beijing during winter, the INP could be assumed to be soot or  
273 ash particles from traffic emissions, biomass burning and coal combustion, or to be dust particles  
274 advected from the desert regions during prevailing northern and north-western wind, or to originate  
275 from the biosphere. Our results indicate that BC particles did not correlate with INP concentrations in  
276 the urban atmosphere. It is possible that the BC particles emitted from coal burning, biomass burning,  
277 and traffic emissions are not ice active in the first place, or that they underwent atmospheric aging  
278 processes (such as coagulation, condensation upon vapor, and chemical reaction) resulting in more  
279 internally mixed particles after emission (Pöschl, 2005), which might inactivate their potential to act as  
280 INP. In the atmosphere of Beijing, the aging timescale is much shorter than in clean environments. For  
281 example, to achieve a complete morphology modification for BC particles in Beijing, the aging  
282 timescale was estimated to be 2.3 h (Peng et al., 2016).  $PM_{2.5}$  chemical composition indicated that the  
283 BC particles may be aged and coated by secondary formed chemical components (SNA and secondary  
284 organic materials) during the heavy haze episodes (Peng et al., 2016), thereby, resulting in weakened  
285 heterogeneous ice nucleation activity of freshly emitted diesel soot particles (Kulkarni et al., 2016).

286 Another study conducted in Ulaanbaatar in Mongolia, a city suffering from severe air pollution,  
287 showed a low ice activity towards heterogeneous ice nucleation when the sulphur content of particles  
288 was highest (Hasenkopf et al., 2016). It is interesting to note that we observe the opposite in our study,  
289 i.e., the increase of  $PM_{2.5}$  mass concentration and percentage of SNA in  $PM_{2.5}$  during haze periods also  
290 seem to have no negative impact on INP concentrations. Not only did increased BC mass  
291 concentrations not increase the observed INP concentrations, but also were INP concentrations not  
292 particularly low during pollution episodes. Furthermore, we conclude that the strong secondary  
293 formation during haze days would not contribute to INP. In addition, there is no clear difference of ice  
294 nucleation between day and night time samples.

295 The size distribution measurements show that the largest fraction of all particles occurred in the  
296 size range below 500 nm. However, during the strongest pollution event towards the end of our  
297 measurement period (Dec. 17 during daytime (1217D) till the night from Dec. 21 to Dec. 22 (1221N)),  
298 also  $N_{>500nm}$  increased noticeably to much larger values than before. In general, also particles in this  
299 size range were affected by the pollution, e.g., by an increase in size of pre-existing particles via



300 atmospheric aging processes (such as coagulation, condensation, chemical reaction) where particles  
301 advected from southern industrial areas of Beijing might also contribute. This is at the base of the  
302 explanation why the parameterizations for  $N_{INP}$  by DeMott et al. (2010, 2015) were not able to describe  
303 the measured values, as seen in Fig. 4 (e) and (f). Indeed, during the pollution phase, the  
304 parameterizations overestimate the observed values by more than two orders of magnitude. But also  
305 during clean phases, neither  $N_{>500nm}$  nor the parameterizations by DeMott et al. (2010, 2015) correlate  
306 with  $N_{INP}$ . Summarizing, this shows that pollution events not only did not add INP, but also that for the  
307 aerosol observed during our study, a parameterization of  $N_{INP}$  based on particles in the size range  $> 500$   
308 nm is not feasible. Interestingly, as will be shortly discussed in the next section, a much older  
309 parameterization by Fletcher (1962) captures  $N_{INP}$  as measured in this study rather surprisingly well, at  
310 least within one order of magnitude (Fig. 5). In summary, during polluted days, the increase of BC  
311 concentration, secondary components (SNA) and other compounds contributing to  $PM_{2.5}$ , as well as  
312 particle concentrations have no impact on INP concentrations down to  $-25^{\circ}C$  in the urban region we  
313 examined in our study. This means that anthropogenic pollution did not contribute to the INP  
314 concentration. But it also indicates that that anthropogenic pollution in Beijing did not deactivate the  
315 present INP, as polluted periods did not show particularly low INP concentrations, although aging and  
316 secondary processes typically are intense during times of strong pollution.

### 317 3.4 Comparison with literature

318 First, we compare our results with results of  $N_{INP}$  derived from precipitation samples as collected  
319 in Petters and Wright (2015) as shown in Fig. 5. These literature data were collected in various  
320 locations in North America and Europe, and none of these locations was one with strong anthropogenic  
321 pollution, different from the sample location in the present study. The  $N_{INP}$  in our study varied from  $10^3$   
322  $-10^4 L^{-1}$  air at the temperature range of  $-10^{\circ}C$  to  $-25^{\circ}C$ . The data of this study (dark green and brownish  
323 lines) are within the range of values given in Petters and Wright (2015), in the whole temperature range  
324 for which INP concentrations were derived here. We also want to point towards the fact that an older  
325 parameterization based on Fletcher (1962), which has been used for large scale modelling, agrees well  
326 with our data (see Fig. 5) down to  $-20^{\circ}C$ . It should, however, also be pointed out that the occurring  
327 variability in the data certainly cannot be captured by such a single line. But the increase in  $N_{INP}$



328 towards lower temperatures as parameterized in Fletcher (1962) is similar to that of our data, where it  
329 should also be said that this parameterization is known to overestimate atmospheric observations at  
330 lower temperatures (roughly below  $-25^{\circ}\text{C}$ , see e.g., Meyers et al., 1992). A similar observation was  
331 recently described in Welti et al. (2017), where down to  $-20^{\circ}\text{C}$  the temperature trend of  $N_{\text{INP}}$  derived  
332 from filter samples taken on the Cape Verde islands also agreed well with the parameterisation by  
333 Fletcher (1962), while at lower temperatures, the parameterization exceeded the measurements. In  
334 general, for the case of the Beijing air masses examined in this study, both the range of  $N_{\text{INP}}$  given in  
335 Petters and Wright (2015) as well as the parameterization by Fletcher (1962) agree better with our  
336 measurements than the parameterizations by DeMott et al. (2010, 2015).

337 All of this is again indicative for the fact that Beijing severe air pollution did not increase or  
338 decrease INP concentrations above or below values typically observed in other, non-urban areas on the  
339 Earth, and hence, that the background INP concentrations, at least down to  $-25^{\circ}\text{C}$  might in general not  
340 be directly anthropogenically influenced.

341 Measurements of  $N_{\text{INP}}$  in China have been done as early as 1963 by You and Shi (1964), and a few  
342 further studies listed in Table 1 have been carried out in recent years. Table 1 includes some campaigns  
343 finished in different regions of China including mountains, plateaus and suburban districts with low  
344  $\text{PM}_{2.5}$  concentration and BC-containing particles. In contrast to these observations, our study shows  
345  $N_{\text{INP}}$  detected in an urban region during highly polluted days with complex particle sources. In our  
346 study, immersion freezing was examined, while not all studies listed in Table 1 examined this ice  
347 nucleation mode. But due to the scarcity of data, we include the results from all these studies in our  
348 discussion here. Apparently, compared with results in Table 1,  $N_{\text{INP}}$  determined for the urban site of  
349 this study ( $1 \text{ L}^{-1}$  Air at  $-20^{\circ}\text{C}$ ) was on the lower end of reported values, which were up to roughly  $20 \text{ L}^{-1}$   
350 Air at  $-20^{\circ}\text{C}$  for non-dust events. Highest concentrations were observed for dust events with values up  
351 to  $604 \text{ L}^{-1}$  ·air at  $-20^{\circ}\text{C}$  detected at a suburban site in Beijing, showing that INP from mineral dust  
352 contribute to the overall  $N_{\text{INP}}$  already at this temperature. Despite the difference among methods and ice  
353 nucleating modes, this again suggests that urban aerosol particles might not be efficient immersion  
354 freezing INP and that the ice nucleating ability of particles in urban aerosols might originate from the  
355 non-urban background aerosol particles that are included in the urban aerosol, i.e., that INP observed in  
356 urban environments might have the same sources among bioaerosols and dust particles as non-urban  
357 INP.



#### 358 4 Conclusions

359 INP concentrations down to  $-25^{\circ}\text{C}$  determined from  $\text{PM}_{2.5}$  samples collected at an urban site of the  
360 megacity Beijing, China, in winter were found to not be influenced by the highly variable amount of air  
361 pollution, both in mass and particle number concentrations, that was present during the sampling  
362 period. Therefore, we conclude that neither BC nor other pollutants contributed to INP, including  
363 secondarily formed particulate mass. On the other hand, we also conclude that the present INP were not  
364 noticeably deactivated during strong pollution events. Particle number concentrations for particles with  
365 diameters  $> 500\text{nm}$  were affected by pollution events, and INP concentrations did not correlate with  
366 these concentrations. Therefore, as can be expected, parameterizations based on these concentrations  
367 DeMott et al. (2010, 2015) do not reproduce the INP concentrations under these extreme conditions  
368 and yield values which are up to more than two orders of magnitude higher than the measured values.  
369 On the other hand, INP concentrations were in the middle of the range reported for atmospheric, non-  
370 urban, concentrations in Petters and Wright (2015), and on the lower end of reported values collected  
371 from previous atmospheric observations in China, while they were much lower than observations  
372 during dust events in China. From this, we conclude that INP concentrations might not be influenced  
373 directly by anthropogenic activities, at least not down to roughly  $-25^{\circ}\text{C}$  and maybe even below, and  
374 that particularly natural mineral dust sources might effect INP concentrations observed in China. It  
375 should be noted that ice nucleation observed at high freezing temperatures (particularly above  $-10^{\circ}\text{C}$ ,  
376 but maybe as low as  $-20^{\circ}\text{C}$ ) is typically attributed to biogenic ice activity. But while identifying the  
377 nature of the INP detected here is beyond the reach of our study, we assume that they originated from  
378 natural sources and not from anthropogenic combustion sources. However, it should be kept in mind  
379 that an indirect anthropogenic influence on INP concentrations is still possible due to land use changes  
380 and related changes in atmospheric dust loadings as well as due to vegetation changes and related  
381 changes in the biosphere.

382

383

#### 384 Appendix

385

##### 386 1. Temperature calibration and background of INDA and LINA

387

388



### 389 **1.1 Temperature calibration of INDA**

390

391 The bath of the thermostat was well mixed during the cooling cycle, and the cooling rate was at 1  
392 K min<sup>-1</sup>. PCR trays were immersed into the cooling liquid such that the water level in the tubes was  
393 below the level of the liquid in the thermostat. The temperature inside the tubes was determined before  
394 the experiments by putting a temperature sensor into a tube during cooling. This was repeated for tubes  
395 in several locations. This worked down to -7°C, below which the sensor induced freezing. In this  
396 temperature range, generally a small constant shift of 0.2 K was observed which was assumed to be  
397 overall valid and was incorporated in the data at all temperatures. A comparison of data obtained for  
398 suspensions of Snomax with previous work done at TROPOS with LACIS (Leipzig Aerosol Cloud  
399 Interaction Simulator) and within INUIT (Ice Nuclei Research Unit, (Wex et al., 2015)) showed good  
400 agreement down to the lowest temperature at which the experiments for the comparison were run,  
401 which was -16°C.

402

### 403 **1.2 Temperature calibration of LINA**

404 The temperature on the glass slide in LINA was obtained by feeding an air flow with a known  
405 dew point temperature through the instrument, while the instrument cooled down with 1 K min<sup>-1</sup>, i.e.,  
406 with the same freezing rate used in the experiments. The humidified air flow was obtained by mixing a  
407 dry air flow with an air flow that was humidified in a Nafion humidifier (Perma Pure MH-110-12S-4,  
408 Perma Pure, Toms River, New Jersey, USA) which was connected to a thermostat (HAAKE C25P,  
409 HAAKE GmbH, Karlsruhe, Germany) that kept the temperature in the humidifier at 10°C. By mixing  
410 the two air streams, dew point temperatures below 0°C were obtained. The dew point temperature was  
411 measured with a dew point mirror (Dew Prime I-S2, Edge Tech, Milford, Massachusetts, USA). The  
412 overall setup is based on the principle of a dew point mirror, i.e., the glass slide on the Peltier element  
413 in LINA started to fog when its temperature reached the dew point temperature adjusted in the air flow.  
414 Optical detection by the CCD camera was deployed similar to how it is used during measurements, i.e.,  
415 taking a picture every 6 s. Subsequently detected greyscale images were compared to an image that  
416 was taken well before fogging began. Brightness differences between this original picture and the  
417 following pictures were taken and resulted in a S-shaped curve, reaching the maximum plateau once  
418 the glass slide was fogged over completely. A fit was applied to the curve in order to find the



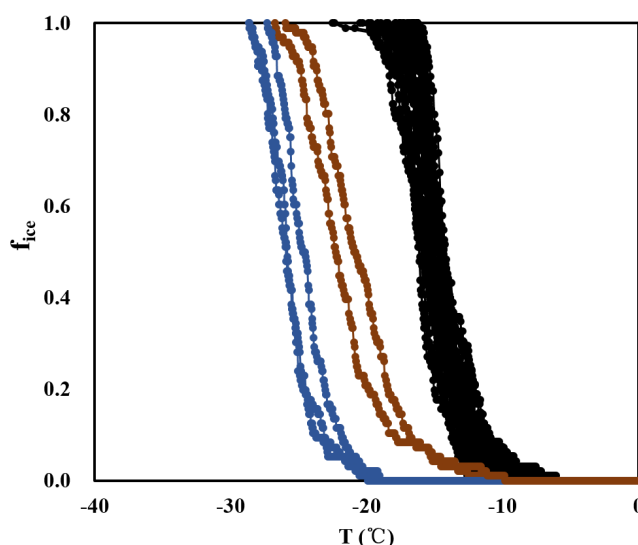
419 temperature where 50% are fogged, which was taken to represent the actual temperature. Using this  
420 principle, the temperature on the glass plate in LINA was calibrated repeatedly at 5 different  
421 temperatures in the range from  $-2.3^{\circ}\text{C}$  to  $-22.3^{\circ}\text{C}$ . A comparison of data obtained for suspensions of  
422 pollen washing water with previous work done at TROPOS with LACIS (Augustin et al., 2013)  
423 showed good agreement down to the lowest temperature at which the experiments for the comparison  
424 were run, which was  $-25^{\circ}\text{C}$ .

425

## 426 2. Background measurement of INDA and LINA

427

428 In the background experiments of INDA, clean filters in distilled water froze from  $-17^{\circ}\text{C}$  to  $-26^{\circ}\text{C}$ ,  
429 while filters with atmospheric particles froze from  $-6^{\circ}\text{C}$  to  $-22^{\circ}\text{C}$ . The  $f_{\text{ice}}$  of the clean filters was 5 to  
430 14 times lower than that of atmospheric samples at the same temperature, showing a low impact. In  
431 LINA measurements, the background of clean filters washed with distilled water was even lower, as  
432 droplets started to freeze at  $-25^{\circ}\text{C}$ . Figure A1 and A2 show the measured frozen fractions of the  
433 samples and the background from pure water and the water with clean filters for both INDA and LINA,  
434 to corroborate that the measurements were well separated from the background.

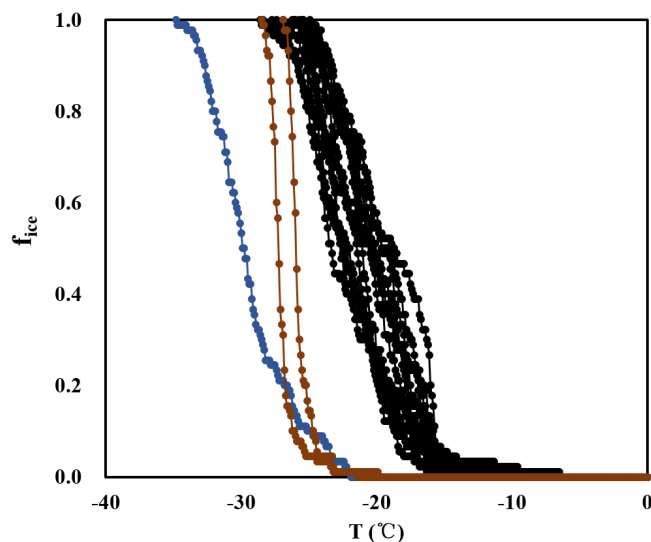


435

436 **Fig. A1 Frozen fractions determined from INDA (black lines), together with background signals determined**  
437 **for pure water (blue lines) and for pure water containing punches of a clean filter (brown lines).**

438





439

440

**Fig. A2** Frozen fractions determined from LINA, together with background signals determined for pure water and for pure water in which a clean filter was put and washed, similar to the procedure for the samples.

441

442

443

444

#### 445 **Acknowledgments**

446

This work is supported by the following projects: National Natural Science Foundation of China

447

(41475127, 41571130021) and Ministry of Science and Technology of the People's Republic of China

448

(2016YFC0202801) and by the DFG funded Ice Nuclei Research Unit (INUIT, FOR 1525) (WE

449

4722/1-2) and Swedish Research Council (639-2013-6917).

#### 450 **References**

451

Alpert, P. A., Aller, J. Y., and Knopf, D. A.: Initiation of the ice phase by marine biogenic surfaces in

452

supersaturated gas and supercooled aqueous phases, *Phys. Chem. Chem. Phys.*, 13, 19882-19894,

453

doi:10.1039/c1cp21844a, 2011.

454

Ansmann, A., Tesche, M., Althausen, D., Müller, D., Seifert, P., Freudenthaler, V., Heese, B.,

455

Wiegner, M., Pisani, G., Knippertz, P., and Dubovik, O.: Influence of Saharan dust on cloud



- 456 glaciation in southern Morocco during the Saharan Mineral Dust Experiment, *J. Geophys. Res.*,  
457 113, doi:10.1029/2007jd008785, 2008.
- 458 Augustin, S., Wex, H., Niedermeier, D., Pummer, B., Grothe, H., Hartmann, S., Tomsche, L., Clauss,  
459 T., Voigtländer, J., Ignatius, K., and Stratmann, F.: Immersion freezing of birch pollen washing  
460 water, *Atmos. Chem. Phys.*, 13, 10989-11003, doi:10.5194/acp-13-10989-2013, 2013.
- 461 Bond, T. C., Doherty, S. J., Fahey, D. W., Forster, P. M., Berntsen, T., DeAngelo, B. J., Flanner, M.  
462 G., Ghan, S., Kärcher, B., Koch, D., Kinne, S., Kondo, Y., Quinn, P. K., Sarofim, M. C., Schultz,  
463 M. G., Schulz, M., Venkataraman, C., Zhang, H., Zhang, S., Bellouin, N., Guttikunda, S. K.,  
464 Hopke, P. K., Jacobson, M. Z., Kaiser, J. W., Klimont, Z., Lohmann, U., Schwarz, J. P., Shindell,  
465 D., Storelvmo, T., Warren, S. G., and Zender, C. S.: Bounding the role of black carbon in the  
466 climate system: A scientific assessment, *J. Geophys. Res.*, 118, 5380-5552,  
467 doi:10.1002/jgrd.50171, 2013.
- 468 Budke, C., and Koop, T.: BINARY: An optical freezing array for assessing temperature and time  
469 dependence of heterogeneous ice nucleation, *Atmos. Meas. Tech.*, 8, 689-703, doi:10.5194/amt-8-  
470 689-2015, 2015.
- 471 Chou, C., Kanji, Z. A., Stetzer, O., Tritscher, T., Chirico, R., Heringa, M. F., Weingartner, E., Prévôt,  
472 A. S. H., Baltensperger, U., and Lohmann, U.: Effect of photochemical ageing on the ice  
473 nucleation properties of diesel and wood burning particles, *Atmos. Chem. Phys.*, 13, 761-772,  
474 doi:10.5194/acp-13-761-2013, 2013.
- 475 Conen, F., Henne, S., Morris, C. E., and Alewell, C.: Atmospheric ice nucleators active  $\geq 12$  °C can  
476 be quantified on PM10 filters, *Atmos. Meas. Tech.*, 5, 321-327, doi:10.5194/amt-5-321-2012,  
477 2012.
- 478 Corbin, J. C., Rehbein, P. J. G., Evans, G. J., and Abbatt, J. P. D.: Combustion particles as ice nuclei in  
479 an urban environment: Evidence from single-particle mass spectrometry, *Atmos. Environ.*, 51,  
480 286-292, doi:<http://dx.doi.org/10.1016/j.atmosenv.2012.01.007>, 2012.



- 481 Cozic, J., Verheggen, B., Mertes, S., Connolly, P., Bower, K., Petzold, A., Baltensperger, U., and  
482 Weingartner, E.: Scavenging of black carbon in mixed phase clouds at the high alpine site  
483 Jungfraujoch, Atmos. Chem. Phys., 7, 11, 2006.
- 484 Cozic, J., Verheggen, B., Mertes, S., Connolly, P., Bower, K., Petzold, A., Baltensperger, U., and  
485 Weingartner, E.: Scavenging of black carbon in mixed phase clouds at the high alpine site  
486 Jungfraujoch, Atmos. Chem. Phys., 7, 1797-1807, doi:10.5194/acp-7-1797-2007, 2007.
- 487 Cozic, J., Mertes, S., Verheggen, B., Cziczo, D. J., Gallavardin, S. J., Walter, S., Baltensperger, U., and  
488 Weingartner, E.: Black carbon enrichment in atmospheric ice particle residuals observed in lower  
489 tropospheric mixed phase clouds, J. Geophys. Res., 113, doi:10.1029/2007jd009266, 2008.
- 490 DeMott, P. J., Sassen, K., Poellot, M. R., Baumgardner, D., Rogers, D. C., Brooks, S. D., Prenni, A. J.,  
491 and Kreidenweis, S. M.: African dust aerosols as atmospheric ice nuclei, Geophys. Res. Lett., 30,  
492 n/a-n/a, 10.1029/2003gl017410, 2003.
- 493 DeMott, P. J., Prenni, A. J., Liu, X., Kreidenweis, S. M., Petters, M. D., Twohy, C. H., Richardson, M.  
494 S., Eidhammer, T., and Rogers, D. C.: Predicting global atmospheric ice nuclei distributions and  
495 their impacts on climate, PNAS, 107, 11217-11222, doi:10.1073/pnas.0910818107, 2010.
- 496 DeMott, P. J., Prenni, A. J., McMeeking, G. R., Sullivan, R. C., Petters, M. D., Tobo, Y., Niemand, M.,  
497 Möhler, O., Snider, J. R., Wang, Z., and Kreidenweis, S. M.: Integrating laboratory and field data  
498 to quantify the immersion freezing ice nucleation activity of mineral dust particles, Atmos. Chem.  
499 Phys., 15, 393-409, doi:10.5194/acp-15-393-2015, 2015.
- 500 DeMott, P. J., Hill, T. C. J., McCluskey, C. S., Prather, K. A., Collins, D. B., Sullivan, R. C., Ruppel,  
501 M. J., Mason, R. H., Irish, V. E., Lee, T., Hwang, C. Y., Rhee, T. S., Snider, J. R., McMeeking, G.  
502 R., Dhaniyala, S., Lewis, E. R., Wentzell, J. J. B., Abbatt, J., Lee, C., Sultana, C. M., Ault, A. P.,  
503 Axson, J. L., Diaz Martinez, M., Venero, I., Santos-Figueroa, G., Stokes, M. D., Deane, G. B.,  
504 Mayol-Bracero, O. L., Grassian, V. H., Bertram, T. H., Bertram, A. K., Moffett, B. F., and Franc,  
505 G. D.: Sea spray aerosol as a unique source of ice nucleating particles, PNAS, 113, 5797-5803,  
506 doi:10.1073/pnas.1514034112, 2016.



- 507 Fröhlich-Nowoisky, J., Hill, T. C. J., Pummer, B. G., Yordanova, P., Franc, G. D., and Pöschl, U.: Ice  
508 nucleation activity in the widespread soil fungus *Mortierella alpina*, *Biogeosciences*, 12, 1057-  
509 1071, doi:10.5194/bg-12-1057-2015, 2015.
- 510 Grawe, S., Augustin-Bauditz, S., Hartmann, S., Hellner, L., Pettersson, J. B. C., Prager, A., Stratmann,  
511 F., and Wex, H.: The immersion freezing behavior of ash particles from wood and brown coal  
512 burning, *Atmos. Chem. Phys.*, 16, 13911-13928, doi:10.5194/acp-16-13911-2016, 2016.
- 513 Guo, S., Hu, M., Guo, Q., Zhang, X., Zheng, M., Zheng, J., Chang, C. C., Schauer, J. J., and Zhang, R.:  
514 Primary sources and secondary formation of organic aerosols in Beijing, China, *Environ. Sci.*  
515 *Technol.*, 46, 9846-9853, doi:10.1021/es2042564, 2012.
- 516 Hang, S., Yan, Y., and Chunsong, L.: Development of new diffusion cloud chamber type and its  
517 observation study of ice nuclei in the Huangshan area., *Chinese Journal of Atmospheric Sciences*,  
518 38, 13, doi:10.3878/j.issn.1006-9895.2013.12211, 2014.
- 519
- 520 Hartmann, S., Augustin, S., Clauss, T., Wex, H., Šantl-Temkiv, T., Voigtländer, J., Niedermeier, D.,  
521 and Stratmann, F.: Immersion freezing of ice nucleation active protein complexes, *Atmos. Chem.*  
522 *Phys.*, 13, 5751-5766, doi:10.5194/acp-13-5751-2013, 2013.
- 523 Hasenkopf, C. A., Veghte, D. P., Schill, G. P., Lodoysamba, S., Freedman, M. A., and Tolbert, M. A.:  
524 Ice nucleation, shape, and composition of aerosol particles in one of the most polluted cities in the  
525 world: Ulaanbaatar, Mongolia, *Atmos. Environ.*, 139, 222-229,  
526 doi:10.1016/j.atmosenv.2016.05.037, 2016.
- 527 Hill, T. C. J., DeMott, P. J., Tobo, Y., Fröhlich-Nowoisky, J., Moffett, B. F., Franc, G. D., and  
528 Kreidenweis, S. M.: Sources of organic ice nucleating particles in soils, *Atmos. Chem. Phys.*, 16,  
529 7195-7211, doi:10.5194/acp-16-7195-2016, 2016.
- 530 Hoose, C., and Möhler, O.: Heterogeneous ice nucleation on atmospheric aerosols: a review of results  
531 from laboratory experiments, *Atmos. Chem. Phys.*, 12, 9817-9854, doi:10.5194/acp-12-9817-  
532 2012, 2012.



- 533 Hu, W., Hu, M., Hu, W.-W., Zheng, J., Chen, C., Wu, Y., and Guo, S.: Seasonal variations of high  
534 time-resolved chemical compositions, sources and evolution for atmospheric submicron aerosols  
535 in the megacity Beijing, Atmos. Chem. Phys. Discuss., 1-43, doi:10.5194/acp-2017-115, 2017.  
536
- 537 Jiang, H., Yin, Y., Yang, L., Yang, S., Su, H., and Chen, K.: The characteristics of atmospheric ice  
538 nuclei measured at different altitudes in the Huangshan Mountains in Southeast China, Adv.  
539 Atmos. Sci., 31, 396-406, doi:10.1007/s00376-013-3048-5, 2014.
- 540 Jiang, H., Yin, Y., Su, H., Shan, Y., and Gao, R.: The characteristics of atmospheric ice nuclei  
541 measured at the top of Huangshan (the Yellow Mountains) in Southeast China using a newly built  
542 static vacuum water vapor diffusion chamber, Atmos. Res., 153, 200-208,  
543 doi:10.1016/j.atmosres.2014.08.015, 2015.
- 544 Jiang, H., Yin, Y., Wang, X., Gao, R., Yuan, L., Chen, K., and Shan, Y.: The measurement and  
545 parameterization of ice nucleating particles in different backgrounds of China, Atmos. Res., 181,  
546 72-80, doi:10.1016/j.atmosres.2016.06.013, 2016.
- 547 Kamphus, M., Ettner-Mahl, M., Klimach, T., Drewnick, F., Keller, L., Cziczo, D. J., Mertes, S.,  
548 Borrmann, S., and Curtius, J.: Chemical composition of ambient aerosol, ice residues and cloud  
549 droplet residues in mixed-phase clouds: single particle analysis during the Cloud and Aerosol  
550 Characterization Experiment (CLACE 6), Atmos. Chem. Phys., 10, 8077-8095, doi:10.5194/acp-  
551 10-8077-2010, 2010.
- 552 Kanji, Z. A., Ladino, L. A., Wex, H., Boose, Y., Burkert-Kohn, M., Cziczo, D. J., and Krämer, M.:  
553 Chapter 1: Overview of Ice Nucleating Particles, Meteorological Monographs,  
554 doi:10.1175/amsmonographs-d-16-0006.1, 2017.
- 555 Kaufmann, L., Marcolli, C., Hofer, J., Pinti, V., Hoyle, C. R., and Peter, T.: Ice nucleation efficiency of  
556 natural dust samples in the immersion mode, Atmos. Chem. Phys., 16, 11177-11206,  
557 doi:10.5194/acp-16-11177-2016, 2016.



- 558 Knopf, D. A., Wang, B., Laskin, A., Moffet, R. C., and Gilles, M. K.: Heterogeneous nucleation of ice  
559 on anthropogenic organic particles collected in Mexico City, *Geophys. Res. Lett.*, 37, n/a-n/a,  
560 doi:10.1029/2010GL043362, 2010.
- 561 Kulkarni, G., China, S., Liu, S., Nandasiri, M., Sharma, N., Wilson, J., Aiken, A. C., Chand, D.,  
562 Laskin, A., Mazzoleni, C., Pekour, M., Shilling, J., Shutthanandan, V., Zelenyuk, A., and Zaveri,  
563 R. A.: Ice nucleation activity of diesel soot particles at cirrus relevant temperature conditions:  
564 Effects of hydration, secondary organics coating, soot morphology, and coagulation, *Geophys.*  
565 *Res. Lett.*, 43, 3580-3588, doi:10.1002/2016gl068707, 2016.
- 566 Levin, E. J. T., McMeeking, G. R., DeMott, P. J., McCluskey, C. S., Carrico, C. M., Nakao, S.,  
567 Jayarathne, T., Stone, E. A., Stockwell, C. E., Yokelson, R. J., and Kreidenweis, S. M.: Ice-  
568 nucleating particle emissions from biomass combustion and the potential importance of soot  
569 aerosol, *J. Geophys. Res.*, 121, 5888-5903, doi:10.1002/2016jd024879, 2016.
- 570 Li, W. J., and Shao, L. Y.: Observation of nitrate coatings on atmospheric mineral dust particles,  
571 *Atmos. Chem. Phys.*, 9, 1863-1871, doi:10.5194/acp-9-1863-2009, 2009.
- 572 Lu, Y., Chi, J., Yao, L., Yang, L., Li, W., Wang, Z., and Wang, W.: Composition and mixing state of  
573 water soluble inorganic ions during hazy days in a background region of North China, *Science*  
574 *China Earth Sciences*, 58, 2026-2033, doi:10.1007/s11430-015-5131-5, 2015.
- 575 Lundheim, R.: Physiological and ecological significance of biological ice nucleators, *Philos Trans R*  
576 *Soc Lond B Biol Sci*, 357, 937-943, doi:10.1098/rstb.2002.1082, 2002.
- 577 Müller, T., Henzing, J. S., de Leeuw, G., Wiedensohler, A., Alastuey, A., Angelov, H., Bizjak, M.,  
578 Collaud Coen, M., Engström, J. E., Gruening, C., Hillamo, R., Hoffer, A., Imre, K., Ivanow, P.,  
579 Jennings, G., Sun, J. Y., Kalivitis, N., Karlsson, H., Komppula, M., Laj, P., Li, S. M., Lunder, C.,  
580 Marinoni, A., Martins dos Santos, S., Moerman, M., Nowak, A., Ogren, J. A., Petzold, A., Pichon,  
581 J. M., Rodriguez, S., Sharma, S., Sheridan, P. J., Teinilä, K., Tuch, T., Viana, M., Virkkula, A.,  
582 Weingartner, E., Wilhelm, R., and Wang, Y. Q.: Characterization and intercomparison of aerosol



- 583           absorption photometers: result of two intercomparison workshops, *Atmos. Meas. Tech.*, 4, 245-  
584           268, doi:10.5194/amt-4-245-2011, 2011.
- 585   Marcolli, C.: Deposition nucleation viewed as homogeneous or immersion freezing in pores and  
586           cavities, *Atmos. Chem. Phys.*, 14, 2071-2104, doi:10.5194/acp-14-2071-2014, 2014.
- 587   Meyers, M. P., Demott, P. J., and Cotton, W. R.: New Primary Ice-Nucleation Parameterizations in an  
588           Explicit Cloud Model, *J. Appl. Meteorol.*, 31, 708-721, 1992.
- 589   Moffett, B. F., Getti, G., Henderson-Begg, S. K., and Hill, T. C. J.: Ubiquity of ice nucleation in lichen  
590           ' possible atmospheric implications, *Lindbergia*, 38, 39-43, 2015.
- 591   Morris, C. E., Conen, F., Alex Huffman, J., Phillips, V., Pöschl, U., and Sands, D. C.: Bioprecipitation:  
592           a feedback cycle linking earth history, ecosystem dynamics and land use through biological ice  
593           nucleators in the atmosphere, *Glob Chang Biol*, 20, 341-351, doi:10.1111/gcb.12447, 2014.
- 594   Murray, B. J., O'Sullivan, D., Atkinson, J. D., and Webb, M. E.: Ice nucleation by particles immersed  
595           in supercooled cloud droplets, *Chem. Soc. Rev.*, 41, 6519-6554, doi:10.1039/c2cs35200a, 2012.
- 596   O'Sullivan, D., Murray, B. J., Ross, J. F., and Webb, M. E.: The adsorption of fungal ice-nucleating  
597           proteins on mineral dusts: a terrestrial reservoir of atmospheric ice-nucleating particles, *Atmos.*  
598           *Chem. Phys.*, 16, 7879-7887, doi:10.5194/acp-16-7879-2016, 2016.
- 599   Pöschl, U.: Atmospheric Aerosols: Composition, Transformation, Climate and Health Effects, *Angew.*  
600           *Chem. Int. Ed.*, 44, 7520-7540, doi:10.1002/anie.200501122, 2005.
- 601   Peng, J., Hu, M., Guo, S., Du, Z., Zheng, J., Shang, D., Levy Zamora, M., Zeng, L., Shao, M., Wu, Y.,  
602           S., Zheng, J., Wang, Y., Glen, C. R., Collins, D. R., Molina, M. J., and Zhang, R.: Markedly  
603           enhanced absorption and direct radiative forcing of black carbon under polluted urban  
604           environments, *PNAS*, 113, 4266-4271, doi:10.1073/pnas.1602310113, 2016.
- 605   Petters, M. D., and Wright, T. P.: Revisiting ice nucleation from precipitation samples, *Geophys. Res.*  
606           *Lett.*, 42, 8758-8766, doi:10.1002/2015GL065733, 2015.



- 607 Pruppacher, H. R., Klett, J. D., and Wang, P. K.: Microphysics of Clouds and Precipitation, *Aerosol*  
608 *Sci. Technol.*, 28, 381-382, doi:10.1080/02786829808965531, 1998.
- 609 Pummer, B. G., Bauer, H., Bernardi, J., Bleicher, S., and Grothe, H.: Suspendable macromolecules are  
610 responsible for ice nucleation activity of birch and conifer pollen, *Atmos. Chem. Phys.*, 12, 2541-  
611 2550, doi:10.5194/acp-12-2541-2012, 2012.
- 612 Pummer, B. G., Budke, C., Augustin-Bauditz, S., Niedermeier, D., Felgitsch, L., Kampf, C. J., Huber,  
613 R. G., Liedl, K. R., Loerting, T., Moschen, T., Schauperl, M., Tollinger, M., Morris, C. E., Wex,  
614 H., Grothe, H., Pöschl, U., Koop, T., and Fröhlich-Nowoisky, J.: Ice nucleation by water-soluble  
615 macromolecules, *Atmos. Chem. Phys.*, 15, 4077-4091, doi:10.5194/acp-15-4077-2015, 2015.
- 616 Rosenfeld, D., Lohmann, U., Raga, G. B., O'Dowd, C. D., Kulmala, M., Fuzzi, S., Reissell, A., and  
617 Andreae, M. O.: Flood or Drought: How Do Aerosols Affect Precipitation?, *Science*, 321, 1309-  
618 1313, doi:10.1126/science.1160606, 2008.
- 619 Schill, G. P., Jathar, S. H., Kodros, J. K., Levin, E. J. T., Galang, A. M., Friedman, B., Link, M. F.,  
620 Farmer, D. K., Pierce, J. R., Kreidenweis, S. M., and DeMott, P. J.: Ice-nucleating particle  
621 emissions from photochemically aged diesel and biodiesel exhaust, *Geophys. Res. Lett.*, 43, 5524-  
622 5531, doi:10.1002/2016gl069529, 2016.
- 623 Schnell, R. C., and Vali, G.: Atmospheric Ice Nuclei from Decomposing Vegetation, *Nature*, 236, 163-  
624 165, 1972.
- 625 Shi, A. Y., Zheng, G. G., and You, L. G.: Observation and analysis on ice nucleus of Henan County of  
626 Qinghai Province in autumn 2003. (in Chinese), *Journal of Applied Meteorological Science*, 17, 5,  
627 2006.
- 628 Szyrmer, W., and Zawadzki, I.: Biogenic and Anthropogenic Sources of Ice-Forming Nuclei: A  
629 Review, *Bulletin of the American Meteorological Society*, 209-209 pp., 1997.
- 630 Umo, N. S., Murray, B. J., Baeza-Romero, M. T., Jones, J. M., Lea-Langton, A. R., Malkin, T. L.,  
631 O'Sullivan, D., Neve, L., Plane, J. M. C., and Williams, A.: Ice nucleation by combustion ash





- 632 particles at conditions relevant to mixed-phase clouds, Atmos. Chem. Phys., 15, 5195-5210,  
633 doi:10.5194/acp-15-5195-2015, 2015.
- 634 Vali: Quantitative Evaluation of Experimental Results on the Heterogeneous Freezing Nucleation of  
635 Supercooled Liquids, Journal of the Atmospheric Science, 28, 8, 1971.
- 636 Vali, G., DeMott, P. J., Möhler, O., and Whale, T. F.: Technical Note: A proposal for ice nucleation  
637 terminology, Atmos. Chem. Phys., 15, 10263-10270, doi:10.5194/acp-15-10263-2015, 2015.
- 638 Welts, A., Müller, K., Fleming, Z. L., and Stratmann, F.: Concentration and variability of ice nuclei in  
639 the subtropic, maritime boundary layer, Atmos. Chem. Phys. Discuss., 2017, 1-18,  
640 doi:10.5194/acp-2017-783, 2017.
- 641 Westbrook, C. D., and Illingworth, A. J.: The formation of ice in a long-lived supercooled layer cloud,  
642 Quarterly Journal of the Royal Meteorological Society, 139, 2209-2221, doi:10.1002/qj.2096,  
643 2013.
- 644 Wex, H., DeMott, P. J., Tobo, Y., Hartmann, S., Rösch, M., Clauss, T., Tomsche, L., Niedermeier, D.,  
645 and Stratmann, F.: Kaolinite particles as ice nuclei: learning from the use of different kaolinite  
646 samples and different coatings, Atmos. Chem. Phys., 14, 5529-5546, doi:10.5194/acp-14-5529-  
647 2014, 2014.
- 648 Wex, H., Augustin-Bauditz, S., Boose, Y., Budke, C., Curtius, J., Diehl, K., Dreyer, A., Frank, F.,  
649 Hartmann, S., Hiranuma, N., Jantsch, E., Kanji, Z. A., Kiselev, A., Koop, T., Möhler, O.,  
650 Niedermeier, D., Nillius, B., Rösch, M., Rose, D., Schmidt, C., Steinke, I., and Stratmann, F.:  
651 Intercomparing different devices for the investigation of ice nucleating particles using Snomax as  
652 test substance, Atmos. Chem. Phys., 15, 1463-1485, doi:10.5194/acp-15-1463-2015, 2015.
- 653 Wilson, T. W., Ladino, L. A., Alpert, P. A., Breckels, M. N., Brooks, I. M., Browse, J., Burrows, S. M.,  
654 Carslaw, K. S., Huffman, J. A., Judd, C., Kilitau, W. P., Mason, R. H., McFiggans, G., Miller, L.  
655 A., Najera, J. J., Polishchuk, E., Rae, S., Schiller, C. L., Si, M., Temprado, J. V., Whale, T. F.,  
656 Wong, J. P. S., Wurl, O., Yakobi-Hancock, J. D., Abbatt, J. P. D., Aller, J. Y., Bertram, A. K.,



- 657 Knopf, D. A., and Murray, B. J.: A marine biogenic source of atmospheric ice-nucleating  
658 particles, *Nature*, 525, 234-238, doi:10.1038/nature14986, 2015.
- 659 Yang, F., Tan, J., Zhao, Q., Du, Z., He, K., Ma, Y., Duan, F., Chen, G., and Zhao, Q.: Characteristics  
660 of PM<sub>2.5</sub> speciation in representative megacities and across China, *Atmos. Chem. Phys.*, 11,  
661 5207-5219, doi:10.5194/acp-11-5207-2011, 2011.
- 662 Yang, L., Yin, Y., Yang, S. Z., Jiang, H., Xiao, H., Chen, Q., Su, H., and Chen, C.: The measurement  
663 and analysis of atmospheric ice nuclei in Nanjing. (in Chinese), *Chinese J. Atmos. Sci*, 37, 11,  
664 doi:10.3878/j.issn.1006-9895.2012.11252 10.3878/j.issn.1006-9895.2012.11242, 2012.
- 665 You, L. G., and Shi, A. Y.: Measurement and analysis of ice-nucleus concentration during the period  
666 from March 18th to April 30th in 1963 in Beijing. (in Chinese), *Acta Meteorologica Sinica*, 34, 7,  
667 1964.
- 668 You, L. G., Yang, S. Z., X.G.Wang, and J.X.Pi: Study of ice nuclei concentration at Beijing in spring  
669 of 1995 and 1996. (in Chinese), *ACTA METEOROLOGICAL SINICA*, 60, 2002.
- 670 Zheng, J., Hu, M., Peng, J., Wu, Z., Kumar, P., Li, M., Wang, Y., and Guo, S.: Spatial distributions and  
671 chemical properties of PM<sub>2.5</sub> based on 21 field campaigns at 17 sites in China, *Chemosphere*,  
672 159, 480-487, doi:10.1016/j.chemosphere.2016.06.032, 2016.
- 673  
674  
675  
676  
677  
678  
679  
680  
681  
682  
683  
684

685 **Table and Figures:**

686

 687 **Table 1. Comparison of INP measurements in different regions of China, including  $N_{INP}$  (i.e., INP number**  
 688 **concentrations) and water vapor saturation ratios with respect to water ( $S_w$ ) (and ice ( $S_i$ ) if explicitly**  
 689 **indicated).**

690

Sampling site	Citation	Sampling Date	Instruments	Temperature (°C) and $S_w$ (%)	Average INP ( $L^{-1}$ Air)	Mode
<b>Huangshan</b> (mountain site)	(Jiang et al., 2015)	September- October,2012	Vacuum water vapor diffusion chamber	-15~-23; $S_i=101\%$	0.27~7.02	Deposition
<b>Huangshan</b> (mountain site)	(Jiang et al., 2014)	May- September,2011	Mixing cloud chamber The static diffusion cloud chamber	-20; $S_w=100\%$	16.6	Deposition/ Condensation
<b>Huangshan</b> (mountain site)	(Hang et al., 2014)	May- September,2011; September- October,2012	Static vacuum water vapor diffusion cloud chamber	-20; $S_i=105\%$ ; $S_w=105\%$	18.74	All modes
<b>Tianshan</b> (mountain site)	(Jiang et al., 2016)	14-24 May, 2014	Vacuum water vapor diffusion chamber; Mixing cloud chamber;	-20; $S_w=100\%$	11(non-dust) Hundreds(dust)	Deposition
<b>Nanjing</b> (suburban site)	(Yang et al., 2012)	May-August,2011	The statistic diffusion chamber;	-20; $S_w=101\%$	20.11	All modes
<b>Qing Hai</b> (plateau site)	(Shi et al., 2006)	5-26 October, 2003	The Bigger mixing cloud chamber	-15, -20, -25	23.3~85.4	Deposition
<b>Beijing</b> (suburban site)	(You and Shi, 1964)	18 March- 30 April,1963	Mixing cloud chamber	-20	3.9~4.8	All modes
<b>Beijing</b> (suburban site)	(You et al., 2002)	18 March- 30 April,1995	The Bigger mixing cloud chamber	-15, -20	21,78.9(non-dust) 604(dust)	All modes
<b>Beijing</b> (urban site)	This study	27 November- 22 December, 2016	Ice Nucleation droplets Array	-10 ~ -28	0.001~10	Immersion

691

692

693

694

695

696

697

698

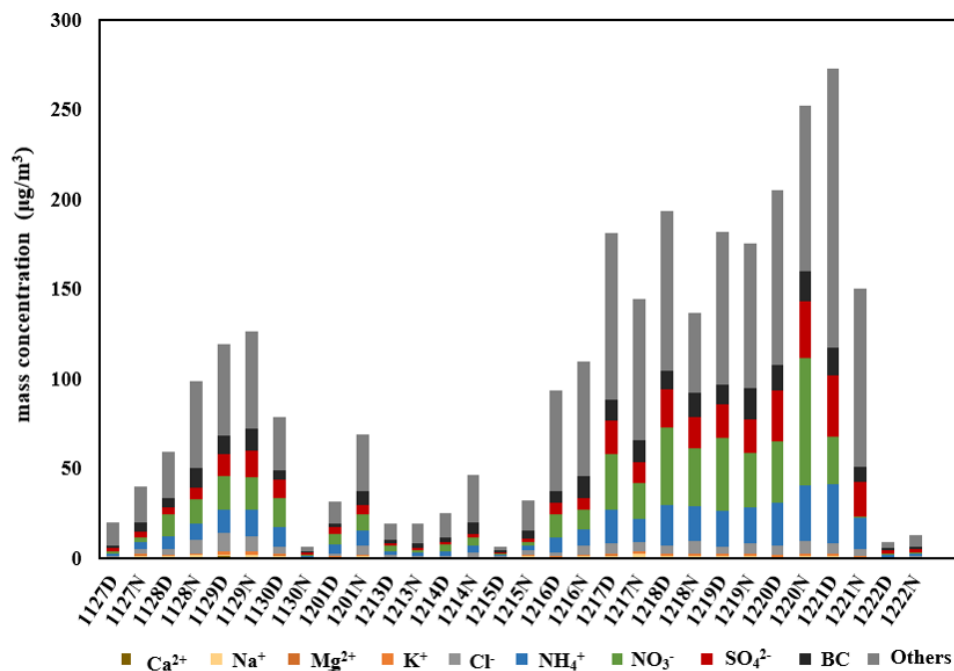
699

700

701

702

703



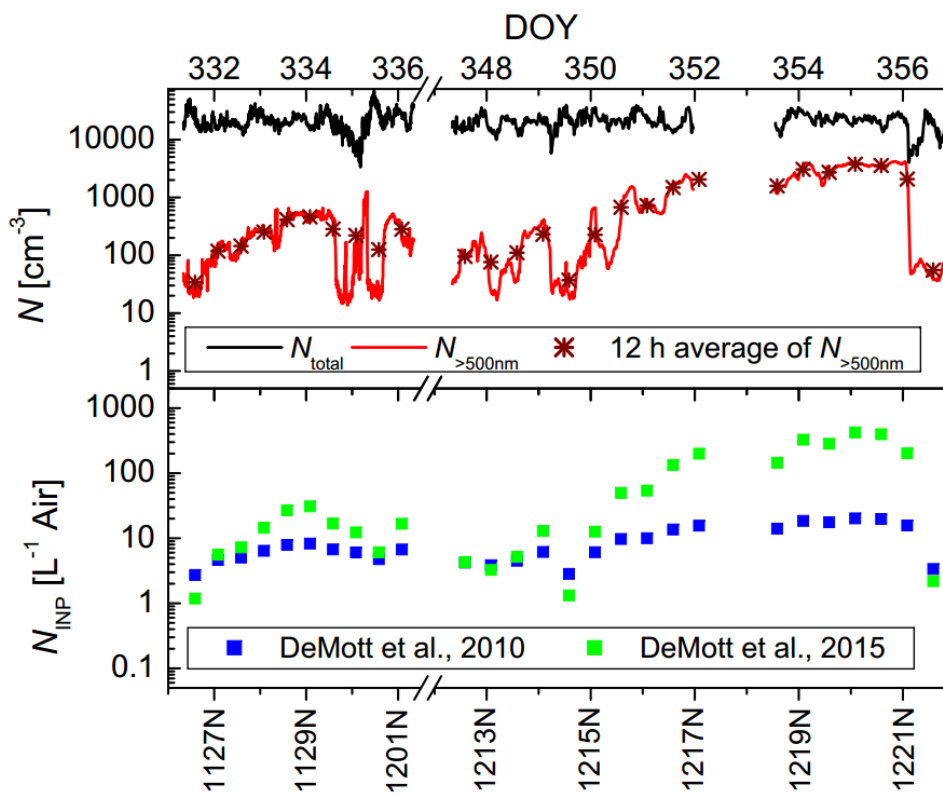
704

705

706

707

**Figure 1.** The time series of  $\text{PM}_{2.5}$  concentrations and chemical composition. Data are shown for 15 different days where the dates are indicated in the x-axis-labeling and “D” and “N” stand for daytime and nighttime, respectively.

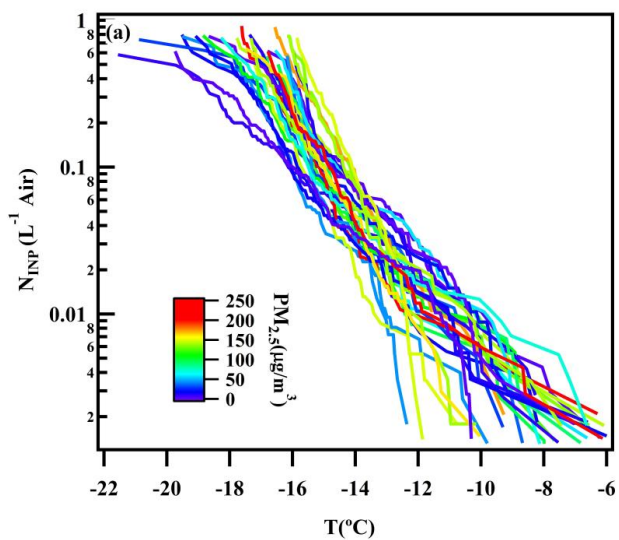


708

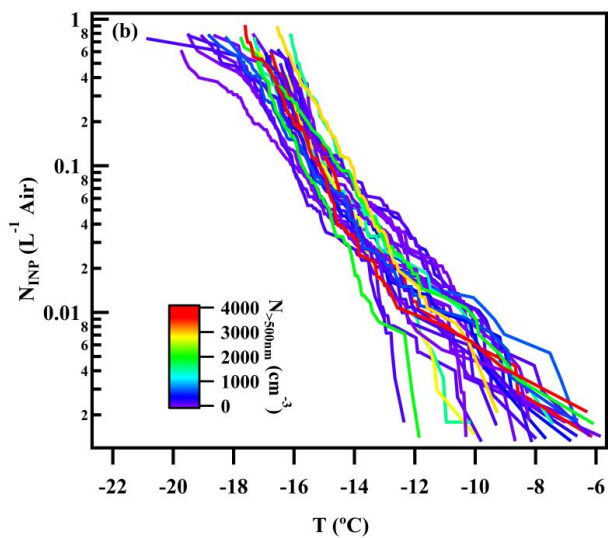
709

710

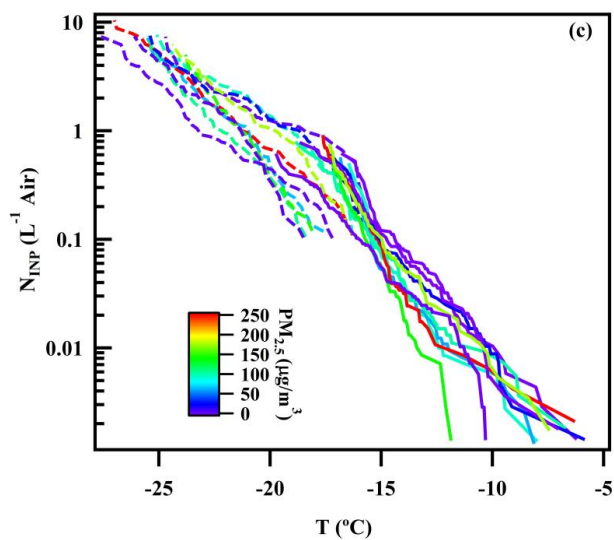
Figure 2. The time series of  $N_{\text{total}}$  and  $N_{>500\text{nm}}$  and the  $N_{\text{INP}}$  parameterized according to DeMott et al. (2010, 2015) at  $-16^\circ\text{C}$ .



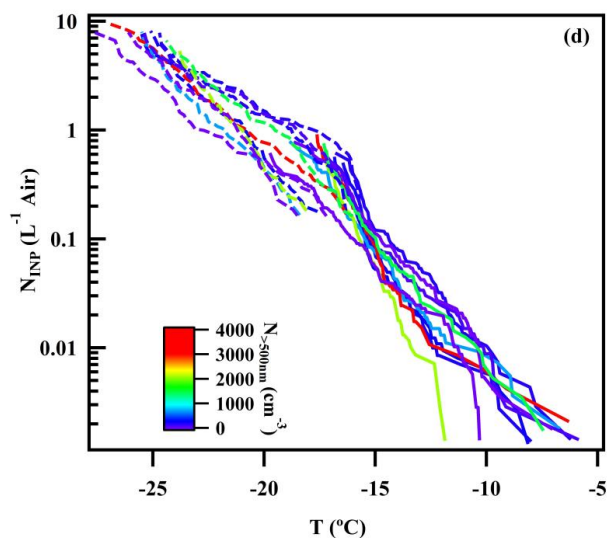
711



712



713

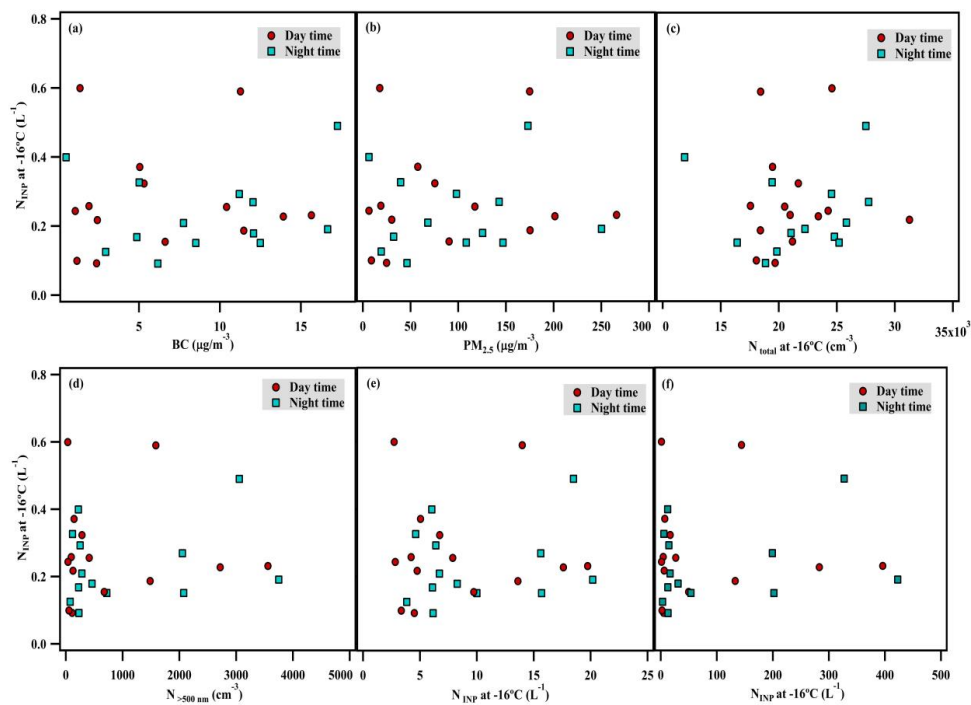


714

715

716 **Figure 3.**  $N_{INP}$  as function of temperature, panel (a) and (b) show INDA results coloured by  $PM_{2.5}$  mass  
717 concentration and 12h-average  $N_{>500nm}$ , (c) and (d) for 10 comparable results of INDA and LINA coloured by  
718  $PM_{2.5}$  mass concentration and 12h-average  $N_{>500nm}$ , solid lines represents LINA results while dashed lines  
719 represents INDA results.

720



721

722

723

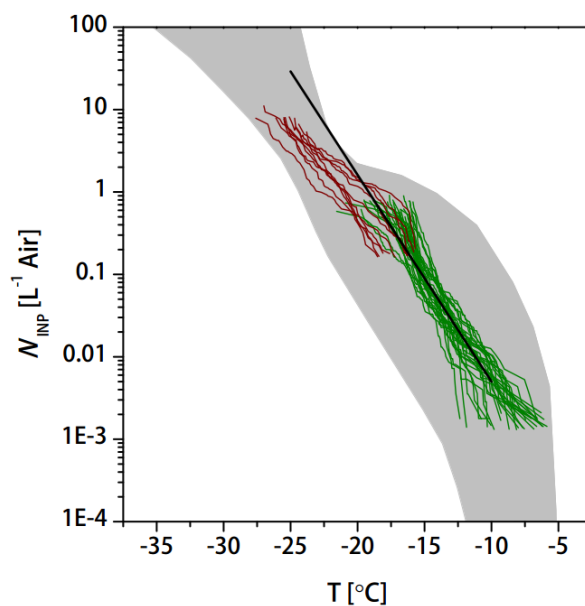
724

725

**Figure 4.**  $N_{INP}$  at  $-16^{\circ}\text{C}$  as function of mass concentrations of BC (a) and  $\text{PM}_{2.5}$  (b), and of 12h-average values of  $N_{total}$  (c). Furthermore, we show  $N_{>500\text{nm}}$  (d), and  $N_{INP}$  at  $-16^{\circ}\text{C}$  derived based on (DeMott et al., 2010) (e) and DeMott et al. (2015) (f) for daytime (red round symbols) and nighttime (green square symbols) samples.

726





727

728 **Figure 5.**  $N_{INP}$  as derived from precipitation samples collected in Petters and Wright (2015) (grey area) and a  
729 parameterization based on Fletcher (1962) (black line), together with our results (dark green and brownish  
730 lines from INDA and LINA-measurements, respectively).

731

732

733